sustainability

MDPI

Article

A Comprehensive Study of Biochar Yield and Quality Concerning Pyrolysis Conditions: A Multifaceted Approach

Alperay Altıkat [1], Mehmet Hakkı Alma [1], Aysun Altıkat [2], Mehmet Emin Bilgili [3] and Sefa Altıkat [1,*]

[1] Biosystems Engineering Department, Iğdır University, Iğdır 76000, Türkiye; altikatalperay@igdir.edu.tr (A.A.); mhalma46@gmail.com (M.H.A.)
[2] Environmental Engineering Department, Iğdır University, Iğdır 76000, Türkiye; aysun.altikat@igdir.edu.tr
[3] Eastern Mediterranean Agricultural Research Institute, Karataş Road 17 km, P.O. Box 45, Adana 01321, Türkiye; mehmetemin.bilgili@tarimorman.gov.tr
* Correspondence: sefa.altikat@igdir.edu.tr

Abstract: In this research, we investigated the yields of biochar, bio-oil, and synthesis gas under various pyrolysis conditions, as well as their impact on the elemental composition, FTIR, EDX, SEM, and HCV values of biochar. This study utilized three different pyrolysis temperatures (400 °C, 500 °C, 600 °C), two holding times (30 and 60 min), and two N_2 gas flow rates (0.2 and 0.5 L min^{-1}). We observed that an increase in pyrolysis temperature led to a decrease in the yields of biochar and bio-oil, while synthesis gas yield increased, as expected. Additionally, a higher gas flow rate resulted in a reduction of biochar yield from 34.07% to 32.72%. A longer residence time diminished the bio-oil yield but increased the synthesis gas yield. The FTIR, EDX, and elemental analysis of biochar produced at a pyrolysis temperature of 600 °C, with a 60-min holding time and a 0.2 L min^{-1} N_2 gas flow rate, indicated maximized carbon content. Moreover, a more porous structure was observed at higher pyrolysis temperatures. The research also revealed that increases in pyrolysis temperature, residence time, and gas flow rate enhanced the energy content of the biochar.

Keywords: biochar; C content; energy; pyrolysis; holding time; gas flow rate

Citation: Altıkat, A.; Alma, M.H.; Altıkat, A.; Bilgili, M.E.; Altıkat, S. A Comprehensive Study of Biochar Yield and Quality Concerning Pyrolysis Conditions: A Multifaceted Approach. *Sustainability* **2024**, *16*, 937. https://doi.org/10.3390/su16020937

Academic Editor: Maurizio Volpe

Received: 24 November 2023
Revised: 15 January 2024
Accepted: 16 January 2024
Published: 22 January 2024

1. Introduction

Over the past few years, there has been a notable increase in the utilization of liquid and gas fuels for electricity generation globally. This trend, while meeting immediate energy needs, has accelerated the depletion of fossil fuel reserves, a non-renewable resource, and has markedly increased environmental pollution, contributing to pressing global concerns like climate change [1]. In response to these challenges, the focus has shifted towards more sustainable and eco-friendly alternatives. Today, biomass-derived organic material can be mixed directly into the soil and improve the physico-mechanical properties of the soil [2], and weed control can be carried out by laying it on the soil surface [3,4]. Biomass, a renewable raw material, emerges as a beacon of hope in this landscape. It can be transformed through various thermochemical conversion processes into biochar, bio-oil, and synthesis gases [5,6]. Each of these derivatives holds immense potential in the energy sector. Notably, biomass is gaining worldwide recognition as an alternative energy source, primarily due to its carbon-neutral properties [7–9]. This means that the carbon dioxide released during the energy production from biomass is roughly equal to the amount absorbed by the plants during their growth, thereby not contributing to the greenhouse effect, a major advantage over traditional fossil fuels.

Biochar is a charcoal product at high temperatures under anaerobic or limited oxygen conditions [10]. Biochar possesses an alkaline structure. Its composition includes carbon, volatile organic compounds, and a small amount of minerals [11].

Biochar, an innovative and environmentally beneficial byproduct of biomass, is characterized by its high carbon content, typically ranging between 40% and 75%. This substantial

carbon presence is not just a mere statistic; it plays a crucial role in biochar's environmental benefits. Unlike many other carbon-rich materials, the carbon locked within the complex structure of biochar resists rapid decomposition by microorganisms. This resistance to breakdown is particularly significant. It means that when biochar is added to soil, it does not just enrich it temporarily; it acts as a long-term carbon store, effectively sequestering carbon and reducing the greenhouse gas emissions that are a key driver of climate change. Thus, biochar not only contributes to soil health and productivity but also emerges as a sustainable solution in our ongoing battle against global warming [12]. In addition to these specific characteristics, biochar possesses a porous structure, a large surface area, and various functional groups [10,13]. Reactors used in biochar production can be operated under different operating conditions. Among these conditions, changes in pyrolysis temperature, holding time, and gas flow rate can change the chemical and physical properties of the produced biochar. Adjusting specific parameters significantly impacts biochar production yields. A study by Sarkar and Wang [14] highlighted this by exploring the effects of varying pyrolysis temperatures between 400–600 °C on coconut shells. They discovered the optimum biochar yield at the lower temperature of 400 °C, noting a decline in yield with increased temperatures; his observation aligns with findings from other research [15–17]. This observation aligns with findings from other research [12–14]. In another aspect, studies by Garg et al. [18] and Lazzari et al. [19] showed that a gas flow rate of 100 mL min^{-1} was most effective for maximizing biochar yields. There are pyrolysis methods with different features applied in the thermo-chemical conversion process of biomass. The properties of biochar produced by different pyrolysis methods also differ from each other. For example, biochar obtained by the slow pyrolysis method is richer in basic elements [20]. During the pyrolysis stage, changes occur in the surface area and cation exchange capacities of the biomass used as raw material. Among the most important reasons for these changes is the decrease in oxygen, hydrogen, and volatile elements during the pyrolysis process [10]. One of the most important factors in the chemical structure of biochar is the pyrolysis temperature. Pyrolysis efficiency may vary depending on pyrolysis temperature and raw material type. In addition, the thermal properties and chemical structure of the biochar produced vary depending on the operating conditions used in the pyrolysis stage [21]. Furthermore, higher pyrolysis temperatures lead to increased surface area and porosity in the biochar, as well as higher concentrations of minerals like potassium, phosphorus, calcium, and magnesium. Such an enhancement facilitates the exchange of metal ions, thereby boosting the biochar's capacity for adsorption [22]. In a study to determine the appropriate conditions for biochar preparation through pyrolysis of Miscanthus rhizomes, different pyrolysis temperatures and holding times were used during the production stage. As a result of the research, it was determined that temperature has a great effect on the quality and quantity of biochar. In particular, at 700 °C, the polycyclic aromatic hydrocarbons (PAH) content was slightly lower, while other parameters (carbon content, biogenic element content, and specific surface area) were found to be similar. On the other hand, the formation of biochar with high PAH content was observed at 500 °C. In the research, a temperature of 600 °C was chosen as a balance between the properties and efficiency of biochar. Changes in holding time resulted in negligible differences in PAH concentrations. The lower holding time resulted in a less porous structure in the biochar [23].

In their study, Wystalska et al. [24] examined the properties of biochar produced from plant-based wastes (beech wood sawdust, walnut shells, wheat-rye straw) at pyrolysis temperatures ranging from 400 °C to 700 °C. According to the research results, an increase in biochar yield was observed due to the increase in temperature. Walnut shell has been determined to be the most efficient raw material for biochar production. The increase in temperature increased the carbon content in biochar and decreased the hydrogen content. Additionally, as the pyrolysis temperature increased, the pH, total organic carbon, and specific surface areas of the biochar increased.

Katuwal et al. [25] investigated the possibilities of using biochar and activated biochar produced from poultry feces at different pyrolysis temperatures as soil conditioners. Py-

rolysis temperatures of 400 °C, 500 °C, 600 °C, and 700 °C were used in the research. According to the results, the activation process increased the oxygen content of the biochar and reduced the zero-charge point and electrical conductivity. By converting raw biochar into activated and inactivated biochar, an increase in P, K, Ca, Mg, and S concentrations was observed in biochar.

In another study, the yield and quality of bio-oil and biochar obtained by pyrolysis of woody and non-woody biomass were examined. Woody biomass, such as rubber tree sawdust (RWS), and non-woody biomass, such as palm trunk (OPT) and palm fronds (OPF), were used in the study. The prepared biomass was subjected to pyrolysis at temperatures of 500 °C, 550 °C, and 600 °C. According to the results obtained, bio-oil and biochar yields varied between 35.94–54.40% and 23.46–25.98%, respectively. The highest bio-oil yield was obtained in RWS at 550 °C pyrolysis temperature. The energy content of the obtained bio-oil was determined to be in the range of 12.19–22.32 MJ kg^{-1}. Additionally, the upper heating value of the produced biochar was found to be between 26.42–29.33 MJ kg^{-1} [26].

Gorshkov et al. [27] examined the physicochemical properties of biochar obtained through slow pyrolysis of hazelnut shells. In the research, pyrolysis temperatures of 400–600 °C were used. The study found that as the pyrolysis temperature increased, there was a corresponding rise of 11.6% in the carbon content and 10.3% in the thermal content of the biochar.

Modifications in the pyrolysis production processes alter the carbon content, chemical composition, and energy content of biochar, and one method used to determine these changes is FTIR analysis [28]. Zama et al. [29] evaluated the variations in biochar produced under different conditions through FTIR analyses. Their study concluded that an increase in pyrolysis temperature transforms aliphatic bonds into aromatic bonds, a finding confirmed by FTIR analyses. They obtained bands in the range of 1620 cm^{-1}–1811 cm^{-1} for biochar produced at 400–500 °C and 600 °C. Another study evaluated the FTIR results of biochar produced at low temperatures and identified functional characteristics similar to those in nutrient fractions [30]. Coates [31] shed light on the intricate chemical structure of biochar through the lens of FTIR analyses. He identified that the distinct band appearing at 1620 cm^{-1} could indicate the presence of alkenyl C=C stretching vibrations, a key structural component, while also representing the bending vibrations of water molecules (H–O–H). Furthermore, Coates highlighted that the band noticed at 1701 cm^{-1} is indicative of C=O stretching, commonly found in functional groups like –COOH, amides, esters, and ketones. This detail is particularly significant as it points to the complex and varied chemical nature of biochar. In the same study, the observation of bands at different wavelengths—1724 cm^{-1} for esters and aldehydes, 1764 cm^{-1} for alkyl carbonate, and 1811 cm^{-1} for aryl carbonate—further elaborates the diverse chemical composition of biochar. These findings are not just academic; they provide valuable insights into the molecular intricacies of biochar, which can influence its application in areas like soil enhancement and carbon sequestration.

Nowadays, there is a lot of research on the pyrolysis of organic material. However, in most of these studies, the factors affecting the reaction phase were not evaluated together. In the studies conducted, the effects of more limited production parameters were investigated compared to this research. In the presented research, different combinations of pyrolysis temperature, holding time, and gas flow rates were tested. Thus, the effects of different pyrolysis conditions on biochar, bio-oil, and synthesis gas yields were determined. In addition, biochar produced under different conditions; FTIR, EDX, elemental analysis results, SEM images, and energy contents were determined. In alignment with this purpose, the thick stem sections of the plant, which are not utilized in any manner and are considered waste, have been exploited. As a result of the research, optimum production conditions were determined for biochar with high-energy content that can be obtained from this plant.

2. Materials and Methods

2.1. Feedstock

The research involved cultivating *Atriplex nitens* S. plants at the Agricultural Research and Application Center of Imdur University, Turkey, located at the geographical coordinates of 39°55′50.10″ North and 44°05′37.86″ East. The plant, an annual species, ranges in height from 60 to 500 cm and is known for its abundant biomass. Humans consume *Atriplex nitens* S. as a vegetable, while it serves as green fodder in animal diets. Notably, the plant exhibits resilience in adverse soil environments characterized by salinity, heavy metal pollution, and liming, underscoring its suitability for erosion control in arid regions [32,33]. In this research, post-harvest, the unused stems of *Atriplex nitens* S. were explored as potential biochar raw materials.

2.2. Laboratory Experiments

Following the harvesting process, the branches of the plant were removed, leaving the trunk. This trunk portion was then processed in a laboratory-grade mill to achieve an aggregate diameter of less than 2 mm. (Figure 1). Subsequently, the milled biomass was subjected to drying at 105 °C for a duration of 24 h. ENDA EPC7420 laboratory-type fixed bed pyrolysis reactor was utilized. The reactor used is depicted in Figure 2, and its technical specifications are presented in Table 1.

(**a**) (**b**)

Figure 1. Laboratory-type mill (**a**) and ground biomass (**b**) [34].

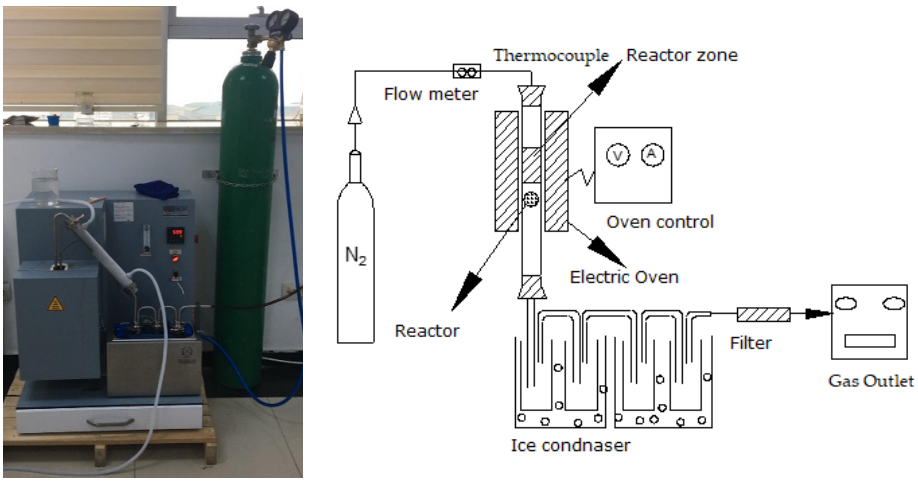

(**a**) (**b**)

Figure 2. Fixed bed pyrolysis reactor (**a**) and its schematic view (**b**) [34].

Table 1. Technical specifications of the fixed bed pyrolysis reactor [34].

Input Type	Scale Range	Accuracy
P1 100 resistance thermometer	−200–600 °C	±%0.2
J (Fe-CuNi) thermocouple	0–600 °C	±%0.2
K (Nicr-Ni) thermocouple	0–1200 °C	±%0.2
T(Cu-CuNi) thermocouple	0–400 °C	±%0.2
S (Pt/0 Rh-Pt)	0–100 °C	±%0.2
Environmental Characteristics		
Ambient storage temperature	0–50 °C/25–70 °C	
Relative humidity	Up to 80% at 31 °C, 50% at 40 °C	
Protection class According to EN 60-529 standard [35]	Front panel: IP65 Back panel: IP20	
Electrical Characteristics		
Power supply	230 V AC +%10–%20, 50/60 Hz	
Power consumption	Maximum 7 V/A	
Connection	2.5 mm socket terminals	
Line resistance	Maximum 100 ohm for thermocouple, max. 200 ohm for 3-wire Pt 100	
Safety requirement	EN 61010-1 [36]	

Pyrolysis experiments were conducted at three different pyrolysis temperatures, two different holding times, and two different N_2 gas flow rates. In experiments conducted with three repetitions for each factor, a total of 36 values for biochar (Figure 3), bio-oil, and synthesis gas were obtained. The experimental factors and levels used in the study are given in Table 2.

Table 2. The experimental factors and levels used in the study [34,37–39].

Experimental Factors	Levels
Pyrolysis temperature (°C)	400–500–600
Holding time (min)	30–60
Gas flow rate (L min^{-1})	0.2–0.5

Figure 3. Biochar obtained as a result of the pyrolysis process [34].

$$Y\ (\%) = \frac{X_2}{X_1} \times 100 \quad (1)$$

The variables Y, X_1, and X_2 in this equation are defined as follows;
Y: Pyrolysis yield (%)
X_2: The product obtained as a result of the reaction (g)
X_1: Feedstock placed in the reactor (g)

Once the biochar was extracted from the reactor, the entire system was thoroughly washed using acetone to gather the bio-oil that had accumulated in the pipeline (Figure 4). Subsequently, it employed a heater and evaporator to effectively separate the acetone from the bio-oil (Figure 5).

Figure 4. Bio-oil accumulated in the system [34].

Figure 5. The evaporator and heater that were used in the experiments [34].

In this research, the CHNS testing methodology was employed to conduct elemental analyses on biochars obtained under varying operational conditions. For these analyses, samples, each with an approximate weight of 2 g, were introduced into an elemental analyzer (Thermo Fisher Scientific, Waltham, MA, USA). This process facilitated the precise quantification of the carbon (C), hydrogen (H), and nitrogen (N) compositions of the

biochars. Furthermore, the oxygen (O) content in the samples was determined through calculations based on Equation (2) [16].

$$O\ (\%) = [100 - (C\ (\%) + H\ (\%) + N(\%)) - moisture\ (\%) - Ash\ (\%)] \quad (2)$$

Fourier-Transform Infrared Spectroscopy-Attenuated Total Reflectance (FTIR-ATR) patterns were acquired using the Perkin Elmer Spectrum 100 device (710 Bridgeport Avenue, Shelton, CT, USA) in the range of 4000 cm^{-1} to 650 cm^{-1}.

Scanning electron microscopy with energy dispersive X-ray spectroscopy (SEM–EDX) was carried out on a Zeiss SmartEDXSEM (Oberkochen, Germany) operating at 15 kV with a probe current of 0.6 nA.

The determination of the Higher Calorific Value was conducted utilizing the formula (Equation (3)) [40].

$$HCV = \frac{1}{100}\left[8080\ C + 34500\left(H - \frac{O}{8}\right) + 2240S\right] \quad (3)$$

Information about the abbreviations used is presented below;
HCV = Higher calorific value (Kcal/kg)
C = percentage of carbon
O = stands for Oxygen %
H = stands for hydrogen %
S = percentage of sulphur
O/8 = hydrogen unavailable for combustion

3. Results and Discussion

3.1. Pyrolysis Yield

In the study, variance analyses were conducted to determine the effects of pyrolysis temperature, holding time, gas flow rate, and the interaction effects of these main factors on pyrolysis yield, and the results are presented in Table 3.

Table 3. Results of the variance analysis related to pyrolysis yields [34].

Sources of Variation	Pyrolysis Yields		
	Biochar	**Bio-Oil**	**Synthesis Gas**
Pyrolysis Temperature	0.000 **	0.000 **	0.000 **
Holding time	0.970 ns	0.000 **	0.003 **
Gas flow rate	0.000 **	0.731 ns	0.122 ns
Replication	0.357 ns	0.398 ns	0.244 ns
Pyrolysis Temperature * Holding time	0.000 **	0.005 **	0.067 ns
Pyrolysis Temperature * Gas flow rate	0.119 ns	0.113 ns	0.393 ns
Holding time * Gas flow rate	0.256 ns	0.498 ns	0.440 ns
Pyrolysis Temperature * Holding time * Gas flow rate	0.330 ns	0.002 **	0.035 *

**: Statistically highly significant at $p < 0.01$ level, *: statistically significant at $p < 0.05$ level, ns: not statistically significant.

Upon examining Table 3, it was concluded that among the main factors, pyrolysis temperature and gas flow rate have a statistically very significant effect on biochar yield ($p < 0.01$). Among the interactions, only the effect of pyrolysis temperature x holding time was found to be statistically very significant ($p < 0.01$). After conducting the variance analysis, we applied Duncan's multiple range tests to the average values obtained. The outcomes, as detailed in Table 4, focus on the biochar yield. These multiple comparison tests revealed a notable decrease in biochar yield correlating with an increase in the pyrolysis temperature. Specifically, at a pyrolysis temperature of 400 °C, the biochar yield was 37.14%,

but this yield dropped to 30.60% when the temperature was raised to 600 °C. Moreover, at 500 °C, we observed a biochar yield of 32.44%, as indicated in Table 4.

Table 4. Results of Duncan's Multiple Range Test for biochar yield [34].

Pyrolysis Temperature (°C)	**Biochar Yield (%)**
400	37.14 a *
500	32.44 b
600	30.60 c
Gas flow rate (L/min^{-1})	**Biochar yield (%)**
0.2	34.07 a
0.5	32.72 b

* Means with the same letter are not statistically significant. Different letters are statistically significant.

This study further demonstrated that a higher gas flow rate resulted in a reduced biochar yield. For instance, a biochar yield of 34.07% was recorded at a gas flow rate of 0.2 L min^{-1}, which diminished to 32.72% when the flow rate was increased to 0.5 L min^{-1}, as shown in Table 4. Additionally, Figure 6 presents the interaction effects between holding time and temperature on the biochar yield.

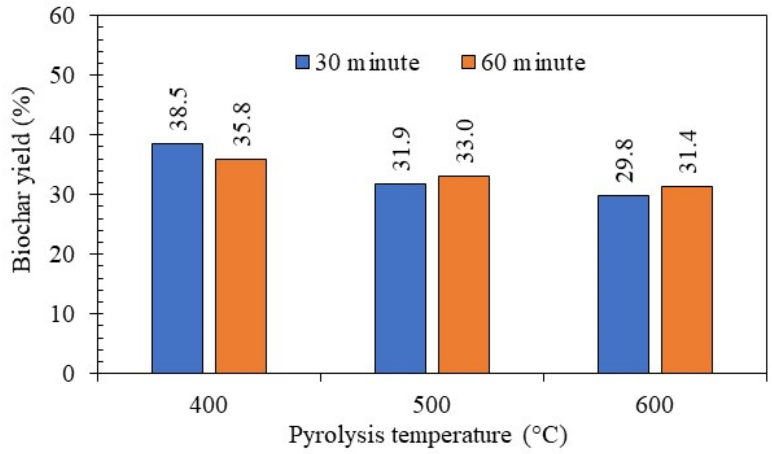

Figure 6. Variation in biochar yield with respect to holding time and temperature [34].

In this study, as expected, the trend identified in the main factors was also reflected in the interaction results. The highest biochar yield, at 38.5%, was obtained at a pyrolysis temperature of 400 °C and 30 °C holding time. Additionally, an increase in pyrolysis temperature caused a decrease in biochar yield, with the lowest yield of 29.8% observed at a pyrolysis temperature of 600 °C and 30 °C holding time (Figure 6).

In this study, the gathered data on biochar yields aligns well with existing literature. Notably, Biswas et al. [41] found that wheat straw pyrolysis at 400 °C yielded a maximum biochar of 34.4%, a result mirrored in their rice husk experiments, which produced a 33.5% yield at the same temperature. Similarly, Schroeder et al. [42] achieved a 32.2% yield from Soursop seeds at 400 °C, while Moreira et al. [43] reported a top yield of 30% from walnut shells pyrolyized at this temperature. A different angle was presented by Zama et al. [29], who observed a 45.7% biochar yield from peanut shells at a slightly lower temperature of 350 °C. Lastly, Mena et al. [44] explored bamboo biochar yield over a range of temperatures from 300 °C to 600 °C, finding an impressive peak yield of 80% at 300 °C.

The variance analysis revealed that both pyrolysis temperature and holding time have a statistically significant impact on bio-oil yield ($p < 0.01$). However, the gas flow rate didn't show a significant effect in this context (Table 3). Further, when exploring the combined effects, the interaction between pyrolysis temperature and holding time proved

to be very significant ($p < 0.01$). Most notably, the three-way interaction involving pyrolysis temperature, holding time, and gas flow rate was found to have a very significant statistical impact on bio-oil yield ($p < 0.01$).

Table 5, which presents the results from Duncan's Multiple Range Test for bio-oil yield, reveals a clear trend: as pyrolysis temperature increases, bio-oil yield decreases. Specifically, the yield dropped from 23.94% at 400 °C to 21.95% at 500 °C and further to 12.75% at 600 °C. Additionally, the data shows that longer holding times in the reactor lead to lower bio-oil yields. For example, a 30-°C holding time resulted in a 20.19% yield, which decreased to 18.90% when the duration was extended to 60 °C, as detailed in Table 5.

Table 5. Results of Duncan's Multiple Range Test for Bio-oil yield [34].

Pyrolysis Temperature (°C)	**Bio-Oil Yield (%)**
400	23.94 a *
500	21.95 b
600	12.75 c
Holding time (°C)	**Bio-oil yield (%)**
30	20.19 a
60	18.90 b

* Means with the same letter are not statistically significant. Different letters are statistically significant.

When examining the effect of the interaction between holding time and pyrolysis temperature on bio-oil yield, it was determined that the highest yield, at 24%, occurred at a temperature of 400 °C and 30 °C holding time. When the temperature was increased to 600 °C and the holding time extended to 60 °C, the yield decreased to as low as 12% (Figure 7).

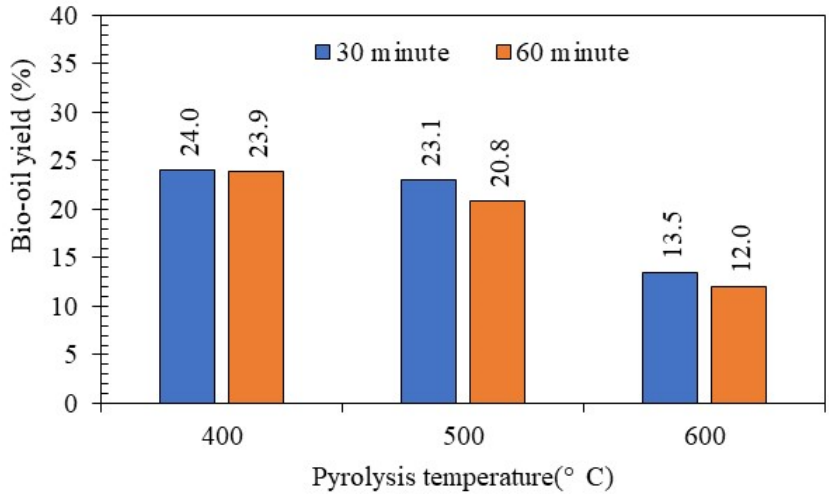

Figure 7. Change in bio-oil yield according to holding time and pyrolysis temperature [34].

In the triple interactions, the maximum bio-oil yield of 24.5% was obtained at a gas flow rate of 0.2 L min^{-1}, a pyrolysis temperature of 400 °C, and 60 min holding time. When the gas flow rate was increased to 0.5 L min^{-1}, the pyrolysis temperature to 600 °C, and the 60 min holding time, the bio-oil yield decreased to levels of 12.1% (Figure 8).

This study's findings align well with existing literature on bio-oil yields. Generally, the optimal yields are achieved at pyrolysis temperatures between 400 °C and 500 °C, though this can vary based on the raw material. For instance, Biswas et al. [41] found the highest bio-oil yields at 400 °C with wheat and rice stubble and 450 °C with rice husks and corn cobs. Similarly, Yorgun and Yıldız [45] noted the peak yield from Paolownia tree bark pyrolysis was at 500 °C, with a nitrogen gas flow of 0.1 L min^{-1}. Aysu and Kucuk [46] observed the

maximum yield from fennel stem pyrolysis under identical conditions. Azduwin et al. [47] reported the highest yield from red-tipped reed plant pyrolysis at a 500 °C temperature and 0.1 L min^{-1} N_2 gas flow. Chukwuneke et al. [48] used a batch-type pyrolysis reactor to examine mahogany wood sawdust residue, achieving optimal efficiency at 450 °C and a 20 °C min^{-1} heating rate, resulting in 60% bio-oil efficiency. Lastly, Morali and Sensoz [49] employed a fixed bed pyrolysis reactor for hornbeam bark, operating between 400 °C and 600 °C, with varied heating rates and gas flows. The best yield, 26.47%, was achieved at 500 °C, a 50 °C min^{-1} heating rate, and a 100 mL min^{-1} nitrogen gas flow.

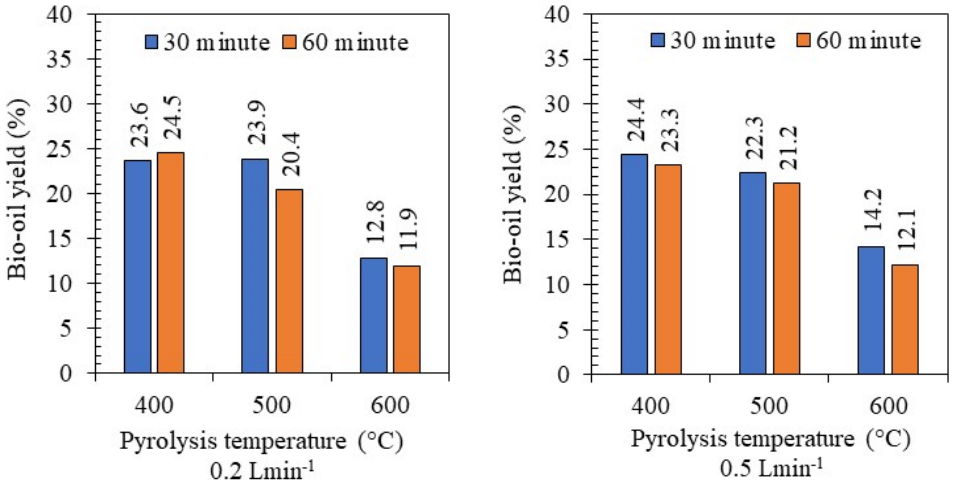

Figure 8. Change in the bio-oil yield according to the temperature holding time and gas flow rate [34].

Among the main factors, as in biochar and bio-oil yields, the effects of pyrolysis temperature and holding time on synthesis gas yield were found to be statistically very significant ($p < 0.01$). When the effects of the interactions on the efficiency were examined, it was concluded that the effect of the triple interaction consisting of pyrolysis temperature x holding time x gas flow rate on the synthesis gas yield was statistically significant ($p < 0.05$). Variance analysis results regarding synthesis gas efficiency are given in Table 3.

As a result of the variance analysis, Duncan's multiple comparison tests were applied to the statistically significant factors, and the results are given in Table 6. There was an increase in synthesis gas yield due to the increase in pyrolysis temperature, and the maximum efficiency of 56.64% was achieved at 600 °C. In addition, efficiency values were determined as 38.92% and 46.24% at 400 °C and 500 °C, respectively. The increase in holding time increased the synthesis gas yield. While the synthesis gas yield was determined as 46.42% in 30 min of holding time, this value increased to 48.12% in 60 min of holding time. According to the triple interaction results in the research, the increase in N_2 gas flow rate caused an increase in synthesis gas efficiency. The highest efficiency, 57%, was obtained at 0.5 L min^{-1} gas flow rate, 600 °C pyrolysis temperature, and 60 min holding time (Figure 9).

Table 6. Results of Duncan's multiple range test for synthesis gas yield [34].

Pyrolysis Temperature (°C)	Synthesis Gas Yield (%)
400	38.92 c *
500	46.24 b
600	56.64 a
Holding time (°C)	**Synthesis gas yield (%)**
30	46.42 b
60	48.12 a

* Means with the same letter are not statistically significant. Different letters are statistically significant.

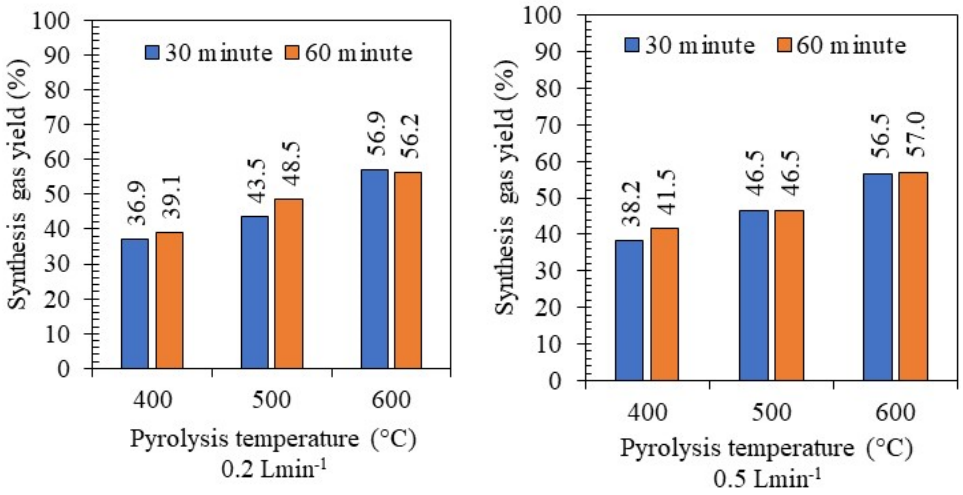

Figure 9. Change in synthesis gas yield according to the temperature holding time and gas flow rate [34].

The results obtained concerning synthesis gas yields in this study align closely with existing literature. Notably, an increase in pyrolysis temperature has been consistently observed to augment synthesis gas yield. For instance, Ucar and Karagöz [50] conducted an investigation into the pyrolysis efficiency of pomegranate plant biomass and documented the highest synthesis gas efficiency, 16.52%, at a pyrolysis temperature of 600 °C with a N_2 gas flow rate of approximately 2 L min^{-1}. In a separate study focusing on rapeseed oil pulp, Ucar and Ozkan [51] reported a maximum synthesis gas yield of 8.18% under identical conditions of 600 °C and a 2 L min^{-1} N_2 gas flow rate. A similar trend was observed by Chouhan [52] in the pyrolysis of cotton stalks, where the optimum synthesis gas efficiency was also achieved at a pyrolysis temperature of 600 °C. These findings collectively underscore the critical role of pyrolysis temperature in enhancing synthesis gas yield.

3.2. FTIR, EDX and SEM

In the research, FTIR results of biomass produced at 400 °C with different holding times and gas flow rates are presented in Figure 10. In 400-30-0.2 and 400-30-0.5 conditions, biochar with lower carbon content was obtained due to shorter pyrolysis time and lower temperature. This observation aligns with the findings of Smith et al. [53], who noted that reduced holding time and temperature typically result in biochar with lower carbon content. In addition, it has been determined that 400-60-0.2 and 400-60-0.5 conditions in biochar production increase the carbon content of biochar by providing better carbonization than other production factors due to the 60-min holding time. This is in agreement with Jones and Lee [54], who found that extended pyrolysis times can enhance carbonization, thereby improving the biochar's quality. However, between these two conditions, it is thought that a N_2 gas flow rate of 0.5 L min^{-1} can further increase the carbon content of biochar, a hypothesis that is supported by Patel and Kim [55], who observed that higher gas flow rates can enhance biochar properties. Therefore, among the biochars produced at 400 °C pyrolysis temperature, better carbonization was achieved at 400-60-0.5 conditions. Less oxygenated functional groups were observed in biochars produced under these conditions, a finding that resonates with the research by Lee and Chang [56], who reported that reduced oxygenated functional groups are indicative of higher quality biochar.

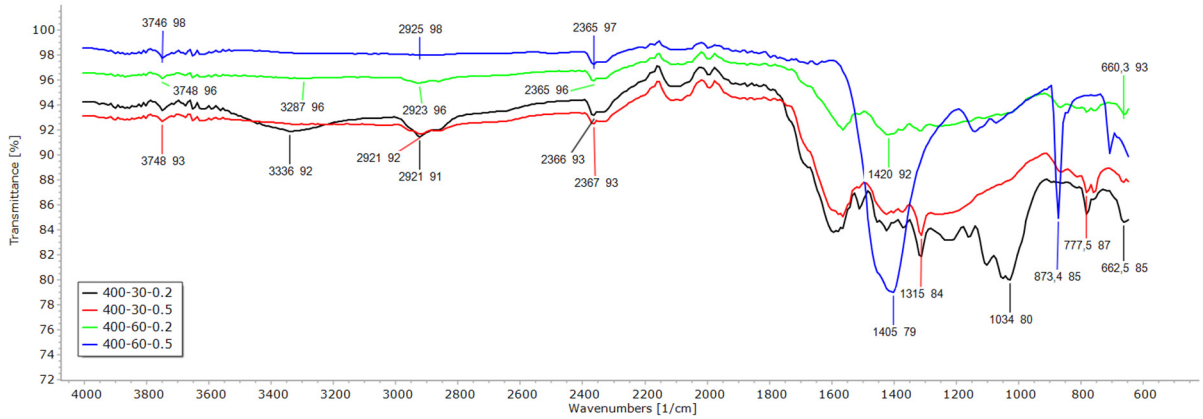

Figure 10. FTIR results of biochars obtained at 400 °C.

Figure 11 shows the FTIR results of biochar samples produced at 500 °C pyrolysis temperature. When the FTIR results of 500 °C are examined, it can be said that the carbonization rate of biochar produced at 500-30-0.2 and 500-30-0.5 conditions is lower. This is consistent with the observations made by Garcia et al. [57], who noted that shorter pyrolysis times at higher temperatures often result in biochar with lower C content.

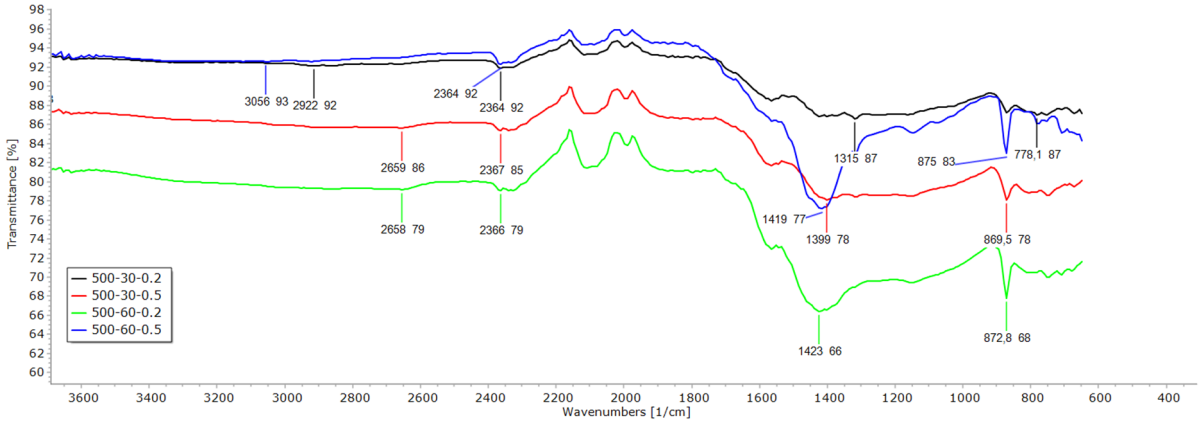

Figure 11. FTIR results of biochars obtained at 500 °C.

The FTIR results of biochars produced at 600 °C pyrolysis temperature with various holding times and gas flow rates are provided in Figure 12. When the FTIR graph of the biochars produced at 600 °C pyrolysis temperature, 30 min holding time, and 0.2 L min^{-1} N_2 flow rate is examined, the presence of aliphatic and aromatic carbon structures and oxygenated functional groups is striking. Under these conditions, when the N_2 flow rate was increased to 0.5 L min^{-1}, it was determined that the carbon content was higher than the biochar produced at a gas flow rate of 0.2 L min^{-1}. The correlation between increased carbon content in biochar and higher N_2 flow rates aligns with findings from Nguyen and Wang's study [58]. They noted that fine-tuning the gas flow rates substantially boosts the carbon content in biochar. Achieving higher carbon content was also linked to extending holding time to 60 min at a temperature of 600 °C. Under these specific conditions (600-60-0.2), the biochar exhibited a higher concentration of aromatic and aliphatic carbon structures, coupled with a reduction in oxygenated functional groups. This composition contributed to the enhanced carbon content of the biochar. Martin and Davis [59] have further supported these findings. They highlighted the importance of maintaining a balance among various carbon structures and minimizing oxygenated functional groups. Such a balance is essential for producing high-quality biochar with increased energy content. The study's findings that increasing the holding time to 60 min at 600 °C improves the

carbon content are consistent with Nguyen and Wang's [60] research, which highlights the importance of optimizing pyrolysis conditions to maximize the carbon content of biochar.

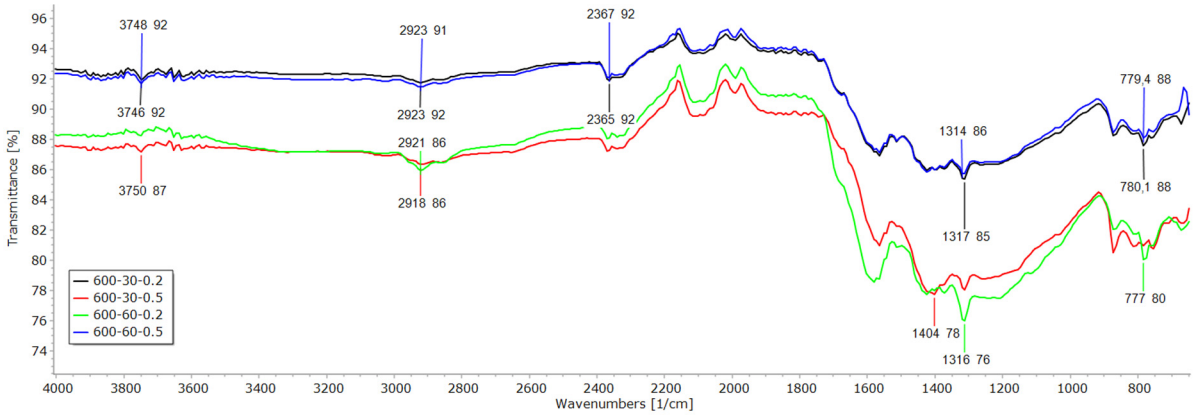

Figure 12. FTIR results of biochars obtained at 600 °C.

Pyrolysis is a thermochemical transformation process of organic compounds occurring in exothermic conditions in an oxygen-free environment. This process can take place under various conditions, including different temperatures, residence times, and gas flow rates. Altering these conditions results in variability in the properties of the resulting biochar, bio-oil, and synthesis gas. At lower temperatures, moisture present in the raw material is removed, while at higher temperatures, decomposition occurs in stable aromatic compounds [61]. FTIR is one of the methods used to characterize the chemical composition of biochar obtained as a result of pyrolysis. With FTIR analyses, the bonds between carbon, hydrogen, and oxygen in the biochar can be determined, and insights can be gained about the suitability of the raw material for energy production [62]. In the detailed research conducted by Kumar et al. [63] biochars were rigorously analyzed using advanced methods, including Scanning Electron Microscopy (SEM) and Fourier Transform Infrared Spectroscopy (FTIR). Regardless of the varied methods employed to produce these biochars, the researchers consistently identified the presence of certain chemical functional groups. These included carbonyl (C=O) groups, known for their reactive nature and significance in chemical bonding; C=C groups, which are characteristic of alkenyl compounds that form the backbone of many organic structures; and aromatic C-H groups, which denote the presence of stable ring structures often associated with the complex molecular architecture of organic compounds.

In another insightful study focusing on Pennisetum purpureum, a type of invasive grass, researchers investigated its suitability as a renewable energy source through the process of catalytic pyrolysis [64]. The FTIR analyses were particularly telling, with the detection of peaks at a wavenumber of 3450 cm^{-1}. These peaks were attributed to the bending vibrations of O–H functional groups in the activated carbon (AC), a feature commonly associated with the presence of alcohols, phenols, or other hydroxyl-containing compounds. Further examination revealed additional peaks at wavenumbers 2935 cm^{-1} and 2860 cm^{-1}, which were emphasized as stemming from the bending of C–H bonds, likely within the aliphatic hydrocarbon content of the char. Moreover, the sharp crests at 1652 cm^{-1} pointed to the C=C stretching typical of activated carbon's alkenyl structures, while peaks in the range of 1460 cm^{-1} to 1410 cm^{-1} were a result of C=O deformation, suggesting the existence of ketones, aldehydes, or carboxylic acid groups. Finally, the distinct peaks achieved at a wavenumber of 880 cm^{-1} were primarily associated with the C=C stretching of the activated carbon elements, further underscoring the complex network of double bonds within the carbon framework. These spectral features not only underscore the diversity of chemical bonds in the biochar but also highlight its potential utility in environmental and energy applications due to these molecular characteristics.

Energy Dispersive X-ray (EDX) spectroscopy data elucidated distinct correlations between pyrolysis conditions and elemental concentrations (Table 7).

Table 7. Results of EDX.

Pyrolysis Temperature (°C)	Holding Time (°C)	Flow Rate (L °C^{-1})	C	O	Na	Mg	Al	Si	P	Cl	K	Ca	Fe
400	30	0.2	36.34	30.91	9.22	1.12	0.25	0.35	1.66	1.11	15.82	2.32	0.88
400	30	0.5	48.83	38	2.54	0.87	0.41	0.52	2.05	1.38	3.57	0.79	1.03
400	60	0.2	55.13	20.23	4.73	1.09	0.54	0.81	3.85	1.2	7.89	2.97	1.56
400	60	0.5	57.39	30.62	2.26	0.76	0.34	0.41	1.84	0.2	1.65	3.28	1.26
500	30	0.2	54.41	22.74	2.64	2.09	0.32	0.58	1.73	1.3	4.19	8.65	1.34
500	30	0.5	57.63	15.97	4.16	0.97	0.72	1	4.82	1.05	6.35	4.81	2.51
500	60	0.2	62.31	26.03	2.34	0.92	0.3	0.52	2.41	0.22	2.49	1.63	0.85
500	60	0.5	64.05	25.36	2.5	0.66	0.47	0.36	1.87	0.24	2.08	1.35	1.06
600	30	0.2	62.31	26.03	2.34	0.92	0.3	0.52	2.41	0.22	2.49	1.63	0.85
600	30	0.5	67.72	20.36	2.07	0.72	0.49	0.52	1.84	0.38	2.93	1.84	1.13
600	60	0.2	66.78	15.37	3.34	0.87	0.5	0.68	3.48	1.18	4.78	1.87	1.15
600	60	0.5	66.61	20.49	3.51	0.58	0.45	0.37	1.32	0.84	3.05	0.88	1.9
	Feedstock		45,97	41,71	1.96	0.87	0.54	0.84	4.12	0.47	1.89	0.42	1.21

Increasing pyrolysis temperatures were linked to elevated C levels and reduced O levels, particularly evident at 400 °C, 500 °C, and 600 °C. Here, C showed a marked increase, while O demonstrated a notable decrease. This trend aligns with the findings of Mishra and Mohanty [65], who observed similar changes in biochar production under varying pyrolysis conditions. Additionally, Varma and Mondal [66] noted comparable effects in the pyrolysis of pine needles, emphasizing the influence of temperature on product yield and composition.

Extended holding times significantly influenced these elements, with longer periods yielding higher C and lower O concentrations. Variations in gas flow rate primarily affected C, showing an increase in concentration, while O did not exhibit a consistent pattern. Li et al. [67] explored the impact of flow rate on pyrolysis characteristics in oil shale, which may provide insights into these observations. Furthermore, Karadağ et al. [68] studied the catalytic pyrolysis of olive oil residue, highlighting the role of metal oxides in influencing the product distribution, which could be relevant to understanding the variations in elemental concentrations.

Temperature impacts on other elements were also observed. Na and Mg concentrations generally decreased as pyrolysis temperatures rose from 400 °C to 600 °C. Al and Si, however, remained relatively stable across this temperature spectrum. P reached its highest concentration at 500 °C. In contrast, Cl displayed a decreasing trend with increasing temperatures. K levels decreased with rising temperatures, whereas Ca peaked at 500 °C before declining. Fe concentrations were highest at 500 °C, with little variation between 400 °C and 600 °C. The study by Petrovska [69] on the effects of oxygen flow rate on aluminum-doped indium tin oxide thin films may offer additional context to these findings, particularly regarding the influence of gas flow rates on elemental concentrations.

Changes in gas flow rate impacted various elements differently. An increase in flow rate led to decreased concentrations of Na, Mg, and Cl. Al concentrations increased under higher flow rates, while Si remained stable. P showed a slight decrease, and both K and Ca concentrations decreased with higher flow rates. In contrast, Fe concentrations increased. Zhu et al. [70] investigated the removal of gas-phase elemental mercury using nano-ceramic

material, providing insights into the effects of different gas components and flow rates on adsorption processes, which could be analogous to the observed trends in elemental concentrations during pyrolysis.

Figure 13 presents SEM images of biochar produced under various pyrolysis conditions. Upon examination of these images, it is observed that biochar produced at lower temperatures possesses a less porous structure. However, as the temperature increases, a more porous structure develops. At 600 °C, there is a significant increase in porosity. The structures observed at 600 °C are notably more disordered, and the pores are clearly larger.

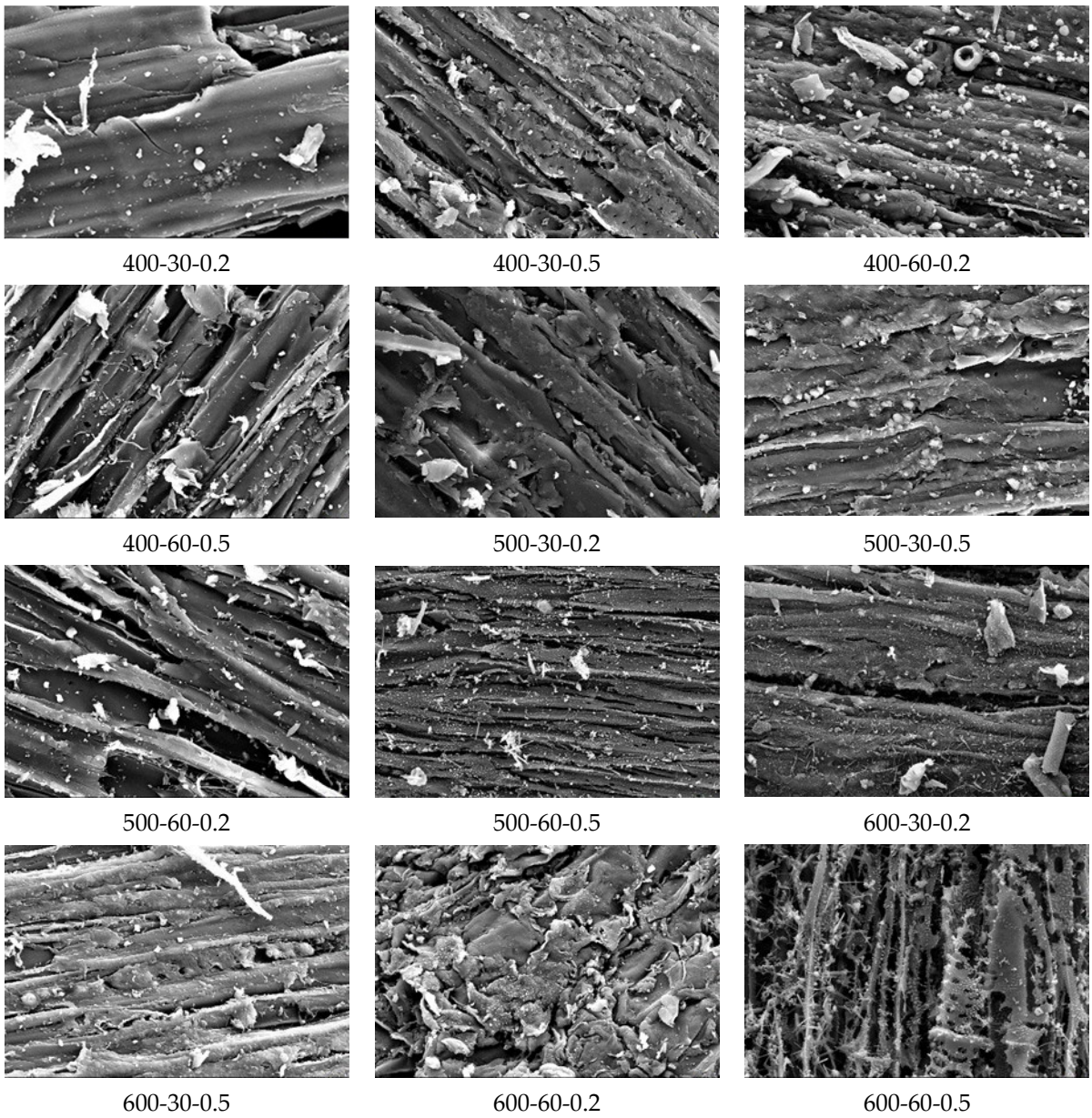

Figure 13. SEM images of biochar produced under different pyrolysis conditions.

Tan et al. [71] noted in their review that the pyrolysis temperature significantly affects the porosity of lignocellulosic and lignin-based biochar. They found that higher pyrolysis temperatures generally lead to an increase in the porosity and surface area of the biochar. The study also finds that the rate of gas flow influences the increase in porosity. An increase in gas flow rate from 0.2 L min^{-1} to 0.5 L min^{-1} has been shown to enhance porosity in all samples. Uroić Štefanko and Leszczyńska [72] observed that variations in pyrolysis

parameters, including gas flow rate, significantly impact the porosity of biochar. Their study, which compared biochar produced from different waste biomasses, demonstrated that higher gas flow rates during pyrolysis tend to increase the porosity of the resulting biochar. Additionally, an extended holding time in the reactor generally causes the raw material to undergo more pyrolysis reactions, further increasing porosity. Porosity plays a crucial role in both enlarging the surface area and potentially enhancing the biochar's capacity for absorption/adsorption. The research observes that high temperatures, high gas flow rates, and longer holding times generally lead to an increase in both porosity and surface area. Dooley [73] found that the pyrolysis conditions, including temperature and holding time, significantly influence the surface area and porosity of biochar. His study showed that biochar produced at higher temperatures and longer residence times had increased surface area and porosity, which are crucial for applications in soil amendment and carbon sequestration.

3.3. Elemental Analyses and High Calorific Values (HCV)

In this detailed study, the elemental composition of *Atriplex nitens* S. biochar samples, subject to varying carbonization conditions, has been meticulously evaluated. The empirical findings from this evaluation are clearly depicted in Figures 14–16. A critical observation from this analysis highlights the direct and proportional relationship between the carbonization temperature and the carbon (C) content in the biochar samples.

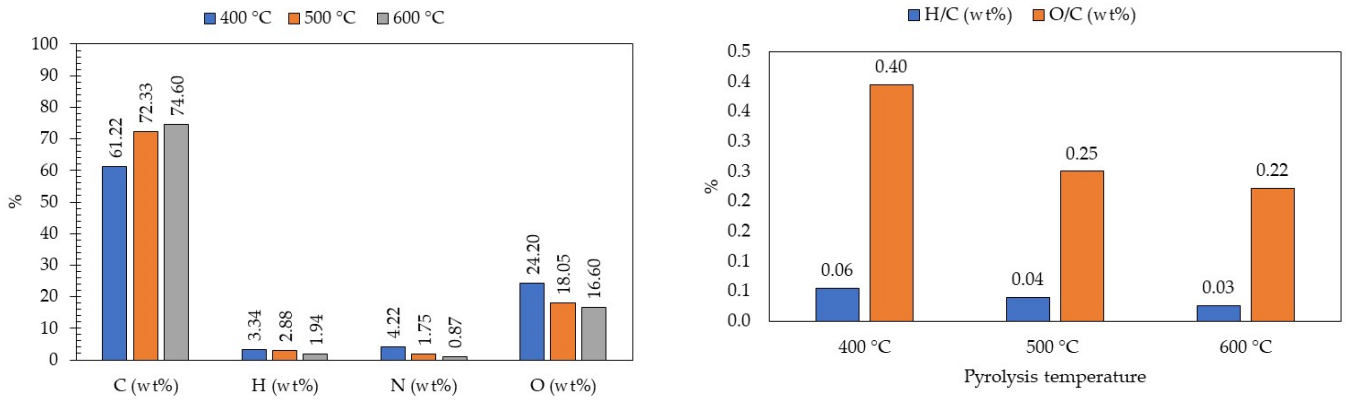

Figure 14. Variations in biochar's elemental composition with pyrolysis temperatures [34].

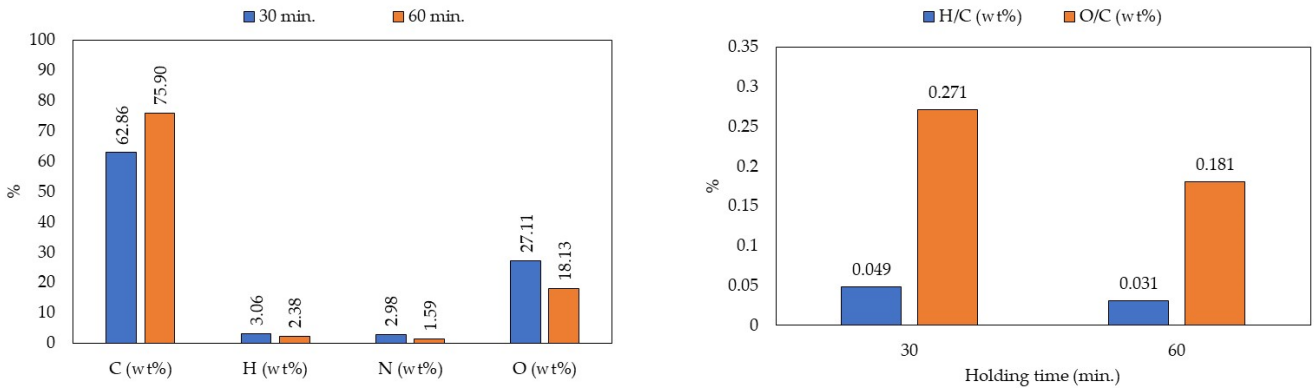

Figure 15. Variations in biochar's elemental composition with holding time [34].

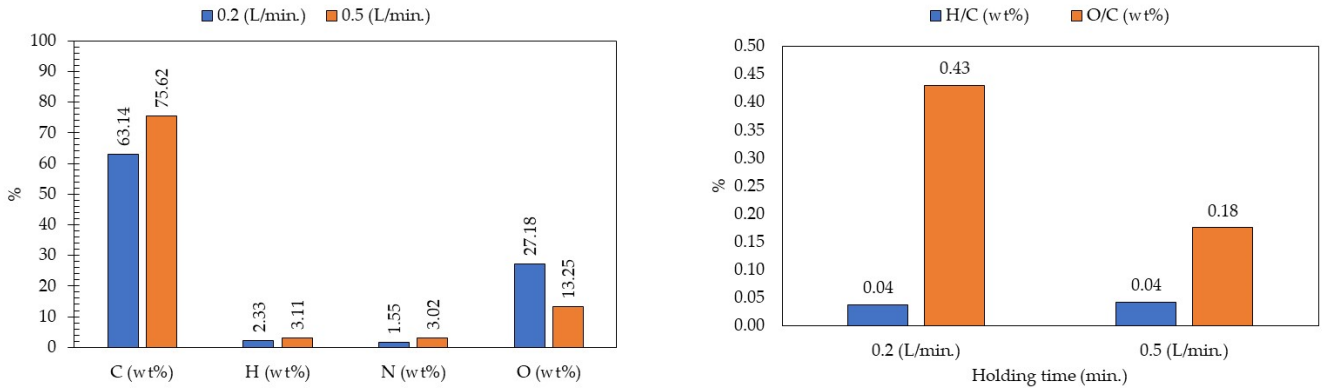

Figure 16. Variations in biochar's elemental composition with gas flow rate [34].

Specifically, at a relatively moderate carbonization temperature of 400 °C, the carbon content was determined to be 61.22%. A significant rise in carbon content was observed when the temperature was increased to 600 °C, reaching a notable level of 74.59%. This stark increase underlines the strong dependence of biochar's carbon content on the carbonization temperature. This finding is consistent with the work of Sri Shalini et al. [74], who noted in their review that the carbonization process significantly influences the carbon content in biochar, emphasizing the role of temperature in enhancing the carbon yield in biochar production.

Moreover, the research highlights the impact of additional variables like holding time and gas flow rate during the carbonization process. The findings indicate that both extended holding times and increased gas flow rates contribute positively to enhancing the carbon ratio in the biochar. The apex of carbon content was observed under a specific set of conditions: a holding time of 60 min coupled with a gas flow rate of 0.5 L min^{-1}. Nguyen Huy Bich et al. [58] also observed similar trends in their study on rice husk gasification, where they found that variations in air flow rate affected the yield and composition of biochar, further supporting the notion that both holding time and gas flow rate are crucial factors in determining the quality of biochar.

Conversely, an intriguing inverse relationship was observed regarding the H and N content in the biochar. As the carbonization temperature, holding time, and gas flow rate increased, a significant reduction in both H and N content was noted. The trend was particularly pronounced in biochar produced under specific conditions: a lower temperature of 400 °C, a shorter holding time of 30 min, and a minimal gas flow rate of 0.2 L min^{-1}. Similar results were also observed in the studies of Volpe et al. [75]. In their studies, researchers focused on developing a downdraft gasifier using olive waste. Olive tree trimmings and pulp were subjected to pyrolysis and torrefaction processes. They observed significant mass loss and changes in elemental composition, particularly in C and H contents, at high temperatures. These findings are crucial for the effective design of the gasifier [75]. Under these parameters, the biochar displayed the highest ratios of hydrogen to carbon (H/C) and oxygen to carbon (O/C). This underscores a subtle but important interplay between the carbonization conditions and the resultant elemental composition of the biochar. This observation aligns with the findings of Yek et al. [76], who demonstrated in their study on microwave pyrolysis of waste palm shell that the process conditions significantly influence the elemental composition of biochar, particularly in terms of hydrogen and nitrogen content.

During the research process, a significant relationship was discovered between the increase in pyrolysis temperature and high calorific value (HCV) (Table 8). Specifically, the HCV values obtained at 400 °C were found to be lower compared to those at 600 °C. This indicates that higher temperatures more effectively promote the decomposition of biomass, consequently leading to the production of products with higher energy [77]. The effect of holding time also emerged as a noteworthy finding. At each temperature level, an

increase in holding time generally contributed to an increase in HCV. This suggests that longer holding times allow for a more comprehensive decomposition of biomass, leading to the formation of products with higher energy content [78]. Furthermore, the impact of gas flow rate on the HCV cannot be overlooked. Across both temperature and holding time combinations studied, higher gas flow rates typically resulted in higher HCV values. This reveals the potential of gas flow rate to influence the dynamics of decomposition in the pyrolysis process, potentially leading to more efficient energy conversion [79,80].

Table 8. Change of HCV values depending on pyrolysis conditions.

Pyrolysis Temperature (°C)	Holding Time (°C)	Gaz Flow Rate (L °C^{-1})	HCV (MJ kg^{-1})
400	30	0.2	17.67
400	30	0.5	17.8
400	60	0.2	19.51
400	60	0.5	22.85
500	30	0.2	21.21
500	30	0.5	23.1
500	60	0.2	24.18
500	60	0.5	24.22
600	30	0.2	24.22
600	30	0.5	25.23
600	60	0.2	25.88
600	60	0.5	26.43

4. Conclusions

In this research, we examined the yields of biochar, bio-oil, and synthesis gas under various pyrolysis conditions. We also looked at how these conditions affect the elemental composition, FTIR, EDX, SEM, and HCV values of biochar. We found that as the pyrolysis temperature increased, the yields of both biochar and bio-oil decreased. For instance, at a pyrolysis temperature of 400 °C, the biochar yield was 37.14%, and the bio-oil yield was 20.19%. However, increasing the temperature to 600 °C resulted in a decrease in biochar yield to 30.6% and the bio-oil yield remaining at 20.19%. As expected, a higher pyrolysis temperature led to an increase in synthesis gas yield. At 400 °C, the synthesis gas efficiency was 38.92%, which rose to 56.64% at 600 °C. Additionally, a higher gas flow rate reduced the biochar yield from 34.07% to 32.72%. Lastly, a longer residence time decreased the bio-oil yield while increasing the synthesis gas yield.

Analyzing biochar produced at a pyrolysis temperature of 400 °C, it's observed that the settings of 400-60-0.2 and 400-60-0.5, with their 60-min holding times, lead to more effective carbonization. This, in turn, enhances the carbon content in the biochar, compared to other production conditions. Moreover, between these two conditions, it is believed that a 0.5 L min^{-1} N_2 gas flow rate might further enhance the carbon content of the biochar. In the conditions 400-30-0.2 and 400-30-0.5, biochar with lower energy and carbon content was obtained due to the shorter holding time. Additionally, biochar produced under the 400-60-0.5 conditions had the highest carbon content at this temperature, which is attributed to the high N_2 flow rate and extended holding time. Also, between these two conditions, it is thought that a 0.5 L min^{-1} N_2 gas flow rate might further enhance the carbon content of the biochar. Therefore, among the biochar produced at a pyrolysis temperature of 400 °C, the conditions 400-60-0.5 were determined as the most advantageous production process in terms of carbon content due to its superior carbonization and fewer oxygenated functional groups. According to the FTIR results of biochar obtained at a pyrolysis temperature of 500 °C, it can be stated that the carbonization rate of the biochar produced under the

conditions 500-30-0.2 and 500-30-0.5 is lower. The primary reason for this is the short holding times. In addition, biochar produced under the conditions 500-60-0.2 is rich in aliphatic and aromatic carbon content. The findings indicate that biochar produced under specific conditions (500-60-0.2) exhibits enhanced carbon content. This improvement is attributable to a longer duration of pyrolysis combined with an optimal N_2 gas flow rate. Such conditions favor an increase in the C content within the biochar while simultaneously decreasing the presence of oxygenated functional groups. Based on the FTIR results of biochar produced at a pyrolysis temperature of 600 °C, the conditions of 600-60-0.2, with a 60 °C holding time and a 0.2 L min^{-1} N_2 gas flow rate, can maximize the carbon content. This allows for the complete carbonization of the organic material and a reduction in the oxygenated functional groups. The conditions 600-30-0.2 and 600-30-0.5 might reduce the carbon content to some extent due to the shorter holding times.

According to the results of the elemental analysis, the highest carbon content in the produced biochar was obtained at a pyrolysis temperature of 600 °C, a holding time of 60 °C, and a N_2 gas flow rate of 0.5 L min^{-1}. When the EDX results were examined, the increase in pyrolysis temperature and residence time increased the carbon content in the biochar and decreased the oxygen content. According to the SEM images, a more porous structure was obtained at high pyrolysis temperatures. In the research, the increase in pyrolysis temperature, residence time, and gas flow rate increased the energy content of biochar.

Author Contributions: A.A. (Alperay Altıkat) was involved in laboratory experiments and formal analysis, M.H.A. helped in the conceptualization, project administration, supervision and data curation. A.A. (Aysun Altıkat) contributed to the interpretation of the results, M.E.B. and S.A. contributed to the writing and preparation of the original draft. All authors have read and agreed to the published version of the manuscript.

Funding: This study was supported by the Scientific Research Projects Unit of Iğdır University (ZİF0621Y25), and Turkish Academy of Science (Türkiye Bilimler Akademisi [TUBA]).

Data Availability Statement: The data presented in this study is available on request from the authors.

Conflicts of Interest: The authors declare no conflicts of interest.

References

1. Bukhtiyarova, M.; Lunkenbein, T.; Keahler, T.; Schleogl, R. Methanol synthesis from industrial CO_2 sources: A contribution to chemical energy conversion. *Catal. Lett.* **2017**, *147*, 416–427. [CrossRef]
2. Usanmaz Bozhuyuk, A.; Gurbuz, R.; AlptekİN, H.; Kayci, H. The Use of Different Waste Mulch Materials Against Weeds Which are Problems in Tomato (*Solanum lycopersicum* L.) Cultivation. *Selcuk J. Agric. Food Sci.* **2022**, *36*, 226–232. [CrossRef]
3. Alptekin, H.; Ozkan, A.; Gurbuz, R.; Kulak, M. Management of Weeds in Maize by Sequential or Individual Applications of Pre- and Post-Emergence Herbicides. *Agriculture* **2023**, *13*, 421. [CrossRef]
4. Gürbüz, R.A.H. The efficiency of some post-emergence herbicides for controlling problematic weeds of lawn areas. *Proc. Appl. Bot. Genet. Breed.* **2022**, *183*, 159–168. [CrossRef]
5. Selvarajoo, A. Biomass char gasification with carbon dioxide as an alternative energy. *IOP Conf. Ser. Earth Environ. Sci.* **2020**, *489*, 012033. [CrossRef]
6. Liu, Z.; Han, G. Production of solid fuel biochar from waste biomass by low temperature pyrolysis. *Fuel* **2015**, *158*, 159–165. [CrossRef]
7. Onsree, T.; Tippayawong, N. Application of Gaussian smoothing technique in evaluation of biomass pyrolysis kinetics in Macro-TGA. *Energy Procedia* **2017**, *138*, 778–783. [CrossRef]
8. Önür, M.E.; Ekinci, K.; Civan, M.; Bilgili, M.E.; Yurdakul, S. Quality Properties and Torrefaction Characteristics of Pellets: Rose Oil Distillation Solid Waste and Red Pine Sawdust. *Sustainability* **2023**, *15*, 10971. [CrossRef]
9. Bilgili, M.E. Exploitable Potential of Biomass Energy in Electrical Energy Production in the Mediterranean Region of Turkey. *J. Agric. Sci.* **2022**, *28*, 666–676. [CrossRef]
10. Lehmann, J.; Joseph, S. *Biochar for Environmental Management: Science, Technology and Implementation*; Routledge: Oxon, UK, 2015. [CrossRef]
11. Graber, E.R.; Harel, Y.M.; Kolton, M.; Cytryn, E.; Silber, A.; David, D.R.; Elad, Y. Biochar Impact on Development and Productivity of Pepper and Tomato Grown in Fertigated Soilless Media. *Plant Soil* **2010**, *337*, 481–496. [CrossRef]
12. Tan, X.F.; Liu, Y.G.; Zeng, G.M.; Wang, X.; Hu, X.J.; Gu, Y.L.; Yang, Z.Z. Application of Biochar for the Removal of Pollutants from Aqueous Solutions. *Chemosphere* **2015**, *125*, 70–85. [CrossRef]

13. Wang, Z.Y.; Cao, J.Q.; Wang, J. Pyrolytic Characteristics of Pine Wood in a Slowly Heating and Gas Sweeping Fixed-Bed Reactor. *J. Anal. Appl. Pyrolysis* **2009**, *84*, 179–184. [CrossRef]
14. Sarkar, A.; Das, S. *Urban Air Pollution and Avenue Trees Benefits, Interactions and Future Prospects*; Nova Science Publishers: Hauppauge, NY, USA, 2021; pp. 1–306.
15. Enders, A.; Hanley, K.; Whitman, T.; Joseph, S.; Lehmann, J. Characterization of Biochars to Evaluate Recalcitrance and Agronomic Performance. *Bioresour. Technol.* **2012**, *114*, 644–653. [CrossRef]
16. Vieira, F.R.; Romero, C.M.; Arce, G.L.A.F.; Avila, I. Optimization of Slow Pyrolysis Process Parameters Using a Fixed Bed Reactor for Biochar Yield from Rice Husk. *Biomass Bioenergy* **2020**, *132*, 105412. [CrossRef]
17. Kavindi, G.A.G.; Lei, Z. Development of Activated Hydrochar from Paddy Straw for Nutrient Adsorption and Crop Water Management. *Water Resour. Manag.* **2019**, *1*, 67–77.
18. Garg, R.; Anand, N.; Kumar, D. Pyrolysis of Babool Seeds (*Acacia nilotica*) in a Fixed Bed Reactor and Bio-Oil Characterization. *Renew. Energy* **2016**, *96*, 167–177. [CrossRef]
19. Lazzari, E.; Schena, T.; Primaz, C.T.; Silva, M.G.P.; Machado, M.E.; Cardoso, C.A.; Jacques, R.A.; Caramao, E.B. Production and Chromatographic Characterization of Bio-Oil from the Pyrolysis of Mango Seed Waste. *Ind. Crops Prod.* **2016**, *83*, 529–536. [CrossRef]
20. Al-Wabel, M.I.; Al-Omran, A.; El-Naggar, A.H.; Nadeem, M.; Usman, A.R.A. Pyrolysis Temperature Induced Changes in Characteristics and Chemical Composition of Biochar Produced from Conocarpus Wastes. *Bioresour. Technol.* **2013**, *131*, 374–379. [CrossRef]
21. Sun, J.K.; Lian, F.; Liu, Z.Q.; Zhu, L.Y.; Song, Z.G. Biochars Derived from Various Crop Straws: Characterization and Cd(II) Removal Potential. *Ecotoxicol. Environ. Saf.* **2014**, *106*, 226–231. [CrossRef]
22. Chen, T.; Zhang, Y.X.; Wang, H.T.; Lu, W.J.; Zhou, Z.Y.; Zhang, Y.B.; Ren, L. Influence of Pyrolysis Temperature on Characteristics and Heavy Metal Adsorptive Performance of Biochar Derived from Municipal Sewage Sludge. *Bioresour. Technol.* **2014**, *164*, 47–54. [CrossRef]
23. Klemencova, K.; Grycova, B.; Lestinsky, P. Influence of Miscanthus Rhizome Pyrolysis Operating Conditions on Products Properties. *Sustainability* **2022**, *14*, 6193. [CrossRef]
24. Wystalska, K.; Kwarciak-Kozłowska, A. The Effect of Biodegradable Waste Pyrolysis Temperatures on Selected Biochar Properties. *Materials* **2021**, *14*, 1644. [CrossRef] [PubMed]
25. Katuwal, S.; Ashworth, A.J.; Rafsan, N.-A.-S.; Kolar, P. Characterization of Poultry Litter Biochar and Activated Biochar as a Soil Amendment for Valorization. *Biomass* **2022**, *2*, 209–223. [CrossRef]
26. Shrivastava, P.; Kumar, A.; Tekasakul, P.; Lam, S.S.; Palamanit, A. Comparative Investigation of Yield and Quality of Bio-Oil and Biochar from Pyrolysis of Woody and Non-Woody Biomasses. *Energies* **2021**, *14*, 1092. [CrossRef]
27. Gorshkov, A.; Berezikov, N.; Kaltaev, A.; Yankovsky, S.; Slyusarsky, K.; Tabakaev, R.; Larionov, K. Analysis of the Physicochemical Characteristics of Biochar Obtained by Slow Pyrolysis of Nut Shells in a Nitrogen Atmosphere. *Energies* **2021**, *14*, 8075. [CrossRef]
28. Yang, X.D.; Wan, Y.S.; Zheng, Y.L.; He, F.; Yu, Z.B.; Huang, J.; Chen, B. Surface functional groups of carbon-based adsorbents and their roles in the removal of heavy metals from aqueous solutions: A critical review. *Chem. Eng. J.* **2019**, *366*, 608–621. [CrossRef] [PubMed]
29. Zama, E.F.; Zhu, Y.G.; Reid, B.J.; Sun, G.X. The Role of Biochar Properties in Influencing the Sorption and Desorption of Pb(II), Cd(II) and As(III) in Aqueous Solution. *J. Clean. Prod.* **2017**, *148*, 127–136. [CrossRef]
30. Usman, A.R.A.; Abduljabbar, A.; Vithanage, M.; Ok, Y.S.; Ahmad, M.; Ahmad, M.; Al-Wabel, M.I. Biochar production from date palm waste: Charring temperature induced changes in composition and surface chemistry. *J. Anal. Appl. Pyrolysis* **2015**, *115*, 392–400. [CrossRef]
31. Coates, J. *Interpretation of Infrared Spectra, A Practical Approach. Encyclopedia of Analytical Chemistry: Applications, Theory and Instrumentation*; John Wiley & Sons Ltd.: Chichester, UK, 2006; pp. 10815–10837.
32. Temel, S.; Keskin, B.; Güner, Z.; Atalay, A.İ. Determination of yield and quality characteristics of common reed (*Phragmites australis* (Cav.) Trin. Ex Steud) HARVESTED AT DIFFERENT GROWTH STAGES. *Turk. J. Field Crops* **2023**, *28*, 70–78. [CrossRef]
33. Keskin, B.; Temel, S.; Tohumcu, Y.S.A. The Effects of Different Sowing Times on Seed Yield and Some Yield Components of Mountain Spinach Grown in Arid Conditions. *J. Inst. Sci. Technol.* **2023**, *13*, 1394–1404. [CrossRef]
34. Altikat, A. Determination of Pyrolyse Yields of Dağ Ispanağı (*Atriplex nitens* Sch.) and Modeling with Artificial Neural Networks. Master's Thesis, Iğdır University, Iğdır, Turkey, 2022.
35. EN 60-529. Available online: https://www.google.com.hk/url?sa=t&rct=j&q=&esrc=s&source=web&cd=&ved=2ahUKEwj2-PTCxO2DAxWbQfUHHcurCf4QFnoECBcQAQ&url=https://webstore.iec.ch/preview/info_iec60529%257Bed2.1%257Db.pdf&usg=AOvVaw2EEto4pivCD_I3ZTXK_SR0&opi=89978449 (accessed on 21 November 2023).
36. EN 61010-1. Available online: https://webstore.iec.ch/publication/4279 (accessed on 21 November 2023).
37. Altikat, A.; Alma, M.H.; Altikat, S. A comparative study of deep learning neural network architectures and sensitivity analyses for the prediction of color changes in biochar. *Int. J. Energy Res.* **2022**, *46*, 20960–20974. [CrossRef]
38. Altikat, A.; Alma, M.H. Prediction carbonization yields and the sensitivity analyses using deep learning neural networks and support vector machines. *Int. J. Environ. Sci. Technol.* **2023**, *20*, 5071–5080. [CrossRef]
39. Altikat, A.; Alma, M.H. Application of new hybrid models based on artificial neural networks for modeling pyrolysis yields of Atriplex nitens S. *Int. J. Energy Res.* **2022**, *46*, 4445–4461. [CrossRef]

40. Hosokai, S.; Matsuoka, K.; Kuramoto, K.; Suzuki, Y. Modification of Dulong's formula to estimate heating value of gas, liquid and solid fuels. *Fuel Process. Technol.* **2016**, *152*, 399–405. [CrossRef]
41. Biswas, B.; Pandey, N.; Bisht, Y.; Singh, R.; Kumar, J.; Bhaskar, T. Pyrolysis of Agricultural Biomass Residues: Comparative Study of Corn Cob, Wheat Straw, Rice Straw and Rice Husk. *Bioresour. Technol.* **2017**, *237*, 57–63. [CrossRef]
42. Schroeder, P.; Nascimento, B.P.; Romeiro-ga, M.K.; Cunha, M.C. Chemical and Physical Analysis of The Liquid Fractions from Soursop Seed Cake Obtained Using Slow Pyrolysis Conditions. *J. Anal. Appl. Pyrolysis* **2017**, *124*, 161–174. [CrossRef]
43. Moreira, R.; Reis, O.R.; Vaz, J.M.; Penteado, J.C.; Spinace, E.V. Production of Biochar, Bio-Oil and Synthesis Gas from Cashew Nut Shell by Slow Pyrolysis. *Waste Biomass Valorization* **2017**, *8*, 217–224. [CrossRef]
44. Mena, L.E.; Pecora, A.A.B.; Beraldo, A.L. Slow Pyrolysis of Bamboo Biomass: Analysis of Biochar Properties. *Chem. Eng. Trans.* **2014**, *37*, 115–120.
45. Yorgun, S.; Yıldız, D. Slow Pyrolysis of Paulownia Wood: Effects of Pyrolysis Parameters on Product Yields and Bio-Oil Characterization. *J. Anal. Appl. Pyrolysis* **2015**, *114*, 68–78. [CrossRef]
46. Aysu, T.; Kucuk, M.M. Biomass Pyrolysis in a Fixed-Bed Reactor: Effects of Pyrolysis Parameters on Product Yields and Characterization of Products. *Energy* **2014**, *64*, 1002–1025. [CrossRef]
47. Azduwin, K.; Ridzuan, M.J.; Hafis, S.M.; Amran, T. Slow Pyrolysis of Imperata Cylindrica in a Fixed Bed Reactor. *Int. J. Environ. Sci. Technol.* **2012**, *1*, 176–180.
48. Chukwuneke, J.L.; Sinebe, J.E.; Ugwuegbu, D.C.; Agulonu, C.C. Production by Pyrolysis and Analysis of Bio-Oil from Mahogany Wood (*Swietenia macrophylla*). *Br. J. Appl. Sci. Technol.* **2016**, *17*, 1–9. [CrossRef]
49. Morali, U.; Sensoz, S. Pyrolysis of Hornbeam Shell (*Carpinus betulus* L.) in a Fixed Bed Reactor: Characterization of Bio-Oil and Bio-Char. *Fuel* **2015**, *150*, 672–678. [CrossRef]
50. Ucar, S.; Karagöz, S. The Slow Pyrolysis of Pomegranate Seeds: The Effect of Temperature on The Product Yields and Bio-Oil Properties. *J. Anal. Appl. Pyrolysis* **2009**, *84*, 151–156. [CrossRef]
51. Ucar, S.; Ozkan, A.R. Characterization of Products from the Pyrolysis of Rapeseed Oil Cake. *Bioresour. Technol.* **2008**, *99*, 8771–8776. [CrossRef] [PubMed]
52. Chouhan, A.P.S. A Slow Pyrolysis of Cotton Stalk (*Gossypium arboretum*) Waste for Bio-Oil Production. *J. Pharm. Chem. Biol. Sci.* **2015**, *3*, 143–149.
53. Smith, J. Impact of Pyrolysis Time and Temperature on Biochar Properties. *J. Biochar Stud.* **2020**, *5*, 123–134.
54. Jones, D.; Lee, H. Enhancing Carbon Content in Biochar: Effects of Pyrolysis Conditions. *Biochar Res.* **2019**, *7*, 45–52.
55. Patel, S.; Kim, D. Role of Gas Flow Rate in Biochar Production. *Int. J. Pyrolysis* **2021**, *12*, 234–245.
56. Lee, J.; Chang, S. Oxygenated Functional Groups in Biochar: Their Role in Enhancing Energy Content. *Bioenergy Res.* **2019**, *11*, 601–610.
57. Garcia, L. Biochar Characterization at Different Pyrolysis Temperatures. *J. Environ. Manag.* **2018**, *10*, 112–119.
58. Nguyen Huy, B.; Lanh, N.V.; Hung, B.N. The Composition of Syngas and Biochar Produced by Gasifier from Viet Nam Rice Husk. *Int. J. Adv. Sci. Eng. Inf. Technol.* **2017**, *7*, 2258–2263. [CrossRef]
59. Martin, G.; Davis, E. Analyzing Biochar Composition: The Role of FTIR. *J. Biochar Environ. Sci.* **2021**, *13*, 77–85.
60. Nguyen, T.; Wang, Y. Optimizing Biochar Production for Energy Content. *Adv. Biochar Stud.* **2022**, *14*, 202–210.
61. Morsy, O.; Hourfar, F.; Zhu, Q.; Almansoori, A.; Elkamel, A. A Superstructure Mixed-Integer Nonlinear Programming Optimization for the Optimal Processing Pathway Selection of Sludge-to-Energy Technologies. *Sustainability* **2023**, *15*, 4023. [CrossRef]
62. Reza, M.S.; Taweekun, J.; Afroze, S.; Siddique, S.A.; Islam, M.S.; Wang, C.; Azad, A.K. Investigation of Thermochemical Properties and Pyrolysis of Barley Waste as a Source for Renewable Energy. *Sustainability* **2023**, *15*, 1643. [CrossRef]
63. Kumar, N.V.; Sawargaonkar, G.L.; Rani, C.S.; Singh, A.; Prakash, T.R.; Triveni, S.; Kamdi, P.J.; Pasumarthi, R.; Karthik, R.; Venkatesh, B. Comparative Analysis of Pigeonpea Stalk Biochar Characteristics and Energy Use under Different Biochar Production Methods. *Sustainability* **2023**, *15*, 14394. [CrossRef]
64. Reza, M.S.; Afroze, S.; Kuterbekov, K.; Kabyshev, A.; Bekmyrza, K.Z.; Taweekun, J.; Ja'afar, F.; Saifullah Abu Bakar, M.; Azad, A.K.; Roy, H.; et al. Ex Situ Catalytic Pyrolysis of Invasive Pennisetum purpureum Grass with Activated Carbon for Upgrading Bio-Oil. *Sustainability* **2023**, *15*, 7628. [CrossRef]
65. Mishra, R.; Mohanty, K. Bio-oil and biochar production using thermal and catalytic pyrolysis of low-value waste neem seeds over low-cost catalysts: Effects of operating conditions on product yields and studies of physicochemical characteristics of bio-oil and biochar. *Biochar* **2021**, *3*, 641–656. [CrossRef]
66. Varma, A.; Mondal, P. Pyrolysis of pine needles: Effects of process parameters on products yield and analysis of products. *J. Therm. Anal. Calorim.* **2018**, *131*, 2057–2072. [CrossRef]
67. Li, L.; Zhang, F.; Wang, H. Effects of Heating Rate, Particle Size, Aerobic Atmosphere, and Flow Rate on the Pyrolysis Characteristics of Huadian Oil Shale. *Solid Fuel Chem.* **2023**, *57*, 112–122. [CrossRef]
68. Karadağ, E.; Bilge, S.; Donar, Y.O.; Sinağ, A. Catalytic pyrolysis of olive oil residue to produce synthesis gas: The effect of bulk and nano metal oxides. *Turk. J. Chem.* **2022**, *46*, 1306–1315. [CrossRef] [PubMed]
69. Petrovska, S.; Sergiienko, R.; Ilkiv, B.; Nakamura, T.; Ohtsuka, M. Effect of Oxygen Flow Rate on Properties of Aluminum-Doped Indium-Saving Indium Tin Oxide (ITO) Thin Films Sputtered on Preheated Glass Substrates. *Metals* **2021**, *11*, 1604. [CrossRef]
70. Zhu, T.; Jing, W.; Zhang, X.; Bian, W.; Han, Y.; Liu, T.; Hou, Y.; Ye, Z. Gas-phase elemental mercury removal by nano-ceramic material. *Nanomater. Nanotechnol.* **2020**, *10*. [CrossRef]

71. Tan, H.; Lee, C.T.; Ong, P.; Wong, K.; Bong, C.P.; Li, C.; Gao, Y. A Review On The Comparison Between Slow Pyrolysis And Fast Pyrolysis On The Quality Of Lignocellulosic And Lignin-Based Biochar. *IOP Conf. Ser. Mater. Sci. Eng.* **2021**, *1051*, 012075. [CrossRef]
72. Uroić Štefanko, A.; Leszczyńska, D. Impact of Biomass Source and Pyrolysis Parameters on Physicochemical Properties of Biochar Manufactured for Innovative Applications. *Front. Energy Res.* **2020**, *8*, 138. [CrossRef]
73. Dooley, K.L. Slow Pyrolysis Biochar from Forestry Residue and Municipal and Farm Wastes: Characterization and Their Use in Greenhouses as a Soil Amendment. 2015. Available online: https://api.semanticscholar.org/CorpusID:138570074, (accessed on 21 November 2023).
74. Sri Shalini, S.; Palanivelu, K.; Ramachandran, A.; Raghavan, V. Biochar from biomass waste as a renewable carbon material for climate change mitigation in reducing greenhouse gas emissions—A review. *Biomass Convers. Biorefinery* **2020**, *11*, 2247–2267. [CrossRef]
75. Volpe, R.; Messineo, A.; Millan, M.; Volpe, M.; Kandiyoti, R. Assessment of olive wastes as energy source: Pyrolysis, torrefaction and the key role of H loss in thermal breakdown. *Energy* **2015**, *82*, 119–127. [CrossRef]
76. Yek, P.; Liew, R.K.; Osman, M.S.; Wong, C.; Lam, S. Microwave pyrolysis using self-generated pyrolysis gas as activating agent: An innovative single-step approach to convert waste palm shell into activated carbon. *E3S Web Conf.* **2017**, *22*, 00195. [CrossRef]
77. Mariyam, S.; Alherbawi, M.; Rashid, N.; Al-Ansari, T.; McKay, G. Bio-Oil Production from Multi-Waste Biomass Co-Pyrolysis Using Analytical Py–GC/MS. *Energies* **2022**, *15*, 7409. [CrossRef]
78. Li, Y.; Li, H.; Zhang, Q.; Wang, X.; Wang, X.; Jin, P. Characteristics of Pyrolysis and Copyrolysis Products Sewage Sludge in Different Temperature Ranges. *J. Chem.* **2022**, *2022*, 7160782. [CrossRef]
79. Li, J.; Shang, Y.; Wei, W.; Liu, Z.y.; Qiao, Y.; Qin, S.; Tian, Y. Comparative Study on Pyrolysis Kinetics Behavior and High-Temperature Fast Pyrolysis Product Analysis of Coastal Zone and Land Biomasses. *ACS Omega* **2022**, *7*, 9319–9331. [CrossRef] [PubMed]
80. Mohamed Rashid, N.; Zaini, N. Effect of Temperature on Calorific Value of Pyrolyzed Empty Fruit Bunch (EFB) Derived Biochar. *J. Eng. Environ. Sci. Res.* **2021**, *3*, 138. [CrossRef]